Semiclassical trace formulae for systems with spin–orbit interactions: successes and limitations of present approaches

2002 J. Phys. A: Math. Gen. 35 6009

(http://iopscience.iop.org/0305-4470/35/29/306)

INSTITUTE OF PHYSICS PUBLISHING JOURNAL OF PHYSICS A: MATHEMATICAL AND GENERAL

J. Phys. A: Math. Gen. **35** (2002) 6009–6032 PII: S0305-4470(02)33909-X

Semiclassical trace formulae for systems with spin–orbit interactions: successes and limitations of present approaches

Ch Amann and M Brack

Institute for Theoretical Physics, University of Regensburg, D-93040 Regensburg, Germany

Received 14 February 2002
Published 12 July 2002
Online at stacks.iop.org/JPhysA/35/6009

Abstract

We discuss the semiclassical approaches for describing systems with spin–orbit interactions. We use these methods to derive trace formulae for several two- and three-dimensional model systems, and exhibit their successes and limitations. We also discuss, in particular, the mode conversion problem that arises in the strong-coupling limit.

PACS numbers: 03.65.Sq, 02.10.De, 05.45.Mt

1. Introduction

The periodic orbit theory (POT) initiated by Gutzwiller over three decades ago [1] has proved to be a successful tool for the semiclassical description of chaotic systems [2–5]. Several extensions of Gutzwiller's semiclassical trace formula to systems with regular and mixed dynamics [6–14] have made it possible to describe quantum shell effects in many physical systems in terms of the shortest classical periodic orbits (see [15, 16] for recent reviews).

However, in all the approaches mentioned so far, the spin degrees of freedom have not been incorporated in the semiclassical theories. This becomes necessary, in particular, when one wants to apply the POT to systems with spin–orbit interactions, such as nuclei, atoms, or semiconductor nanostructures. Littlejohn and Flynn [17] have developed a semiclassical theory of systems with multi-component wavefunctions and applied this [18] to the WKB quantization of integrable spherical systems with the standard spin–orbit interaction; Frisk and Guhr [19] have extended their method to deformed systems with spin–orbit interaction. However, none of these authors have developed an explicit trace formula. Bolte and Keppeler [20] have recently derived a relativistic trace formula from the Dirac equation. They studied several non-relativistic limits and rederived the Littlejohn–Flynn (LF) approach in the limit of a strong spin–orbit coupling, thereby justifying some ad hoc assumptions made in [19]. A problem that has remained unsolved in the strong-coupling limit is that of the so-called mode conversion: the semiclassical description breaks down at those points (or subspaces) of the classical phase space where the spin–orbit interaction locally becomes zero.

0305-4470/02/296009+24$30.00

In the present paper, we shall apply the above methods to various two- and three-dimensional model systems, test their ability to reproduce the coarse-grained quantum-mechanical level densities of these systems, and explore their limitations. We shall also discuss the mode conversion problem that arises in the strong-coupling limit. Some preliminary results of our investigations have been presented in [21, 22].

This paper is organized as follows. After a short reminder of semiclassical trace formulae for coarse-grained quantum systems in section 2, we review in section 3 the approaches of [17, 19, 20] which we then apply in the following. In section 4.1 we investigate the two-dimensional electron gas (2DEG) with a spin–orbit interaction of Rashba type in an external magnetic field. In section 4.2 we add to this system a laterally confining anisotropic harmonic-oscillator potential as a model for an anisotropic semiconductor quantum dot. Section 5 is devoted to a three-dimensional harmonic-oscillator potential with standard spin–orbit interaction of Thomas type, as in the shell model for light atomic nuclei (see, e.g., [23]). In section 6, we finally discuss the mode conversion problem and present some supporting evidence for the diabatic spin–flip hypothesis proposed in [19].

2. Trace formulae with coarse-graining

The primary object of the semiclassical trace formulae is the level density (or density of states)

$$g(E) = \sum_k \delta(E - E_k) \tag{1}$$

of a system described quantum-mechanically by the stationary Schrödinger equation

$$\widehat{H}\phi_k = E_k\phi_k. \tag{2}$$

We stay throughout in the non-relativistic limit and assume the energy spectrum $\{E_k\}$ to be discrete. Classically, the system is described by a Hamilton function $H(\boldsymbol{r}, \boldsymbol{p}) = E$ and the equations of motion derived from it. The function $H(\boldsymbol{r}, \boldsymbol{p})$ may be understood as the phase-space symbol of the operator $\widehat{H}$ in the limit $\hbar \to 0$.

The level density (1) can be written as a sum of a smooth part and an oscillating part:

$$g(E) = \widetilde{g}(E) + \delta g(E). \tag{3}$$

The smooth part $\widetilde{g}(E)$ is given by the contribution of all orbits with zero length [25] in the POT. It is often easily evaluated by the (extended) Thomas–Fermi theory or by a numerical Strutinsky averaging [26] of the quantum spectrum (see [15] for the relation of all three methods). The oscillating part $\delta g(E)$ is semiclassically approximated by trace formulae of the form

$$\delta g_{sc}(E) = \sum_{po} \mathcal{A}_{po}(E) \cos\left(\frac{1}{\hbar} S_{po}(E) - \frac{\pi}{2}\sigma_{po}\right). \tag{4}$$

The sum here is over all periodic orbits (po) of the classical system, including all repetitions of each primitive periodic orbit (ppo). $S_{po}(E)$ is the action integral and σ_{po} the so-called Maslov index of a periodic orbit. The amplitude $\mathcal{A}_{po}(E)$ depends on the integrability and the continuous symmetries of the system. When all periodic orbits are isolated in phase space, the amplitude is given by [1]

$$\mathcal{A}_{po}(E) = \frac{1}{\pi\hbar} \frac{T_{ppo}}{\sqrt{|\det(\widetilde{\mathbb{M}}_{po} - \mathbb{1})|}} \tag{5}$$

where T_{ppo} is the period of the primitive orbit and $\widetilde{\mathbb{M}}_{po}$ the stability matrix of the periodic orbit. The examples of amplitude factors for systems with continuous symmetries or for integrable systems may be found in the introduction.

The *po* sum in (4) does not converge in most cases; it must, in general, be understood as an asymptotic series that is only semiconvergent. However, much practical use can be made of trace formulae if one does not attempt to obtain an exact energy spectrum (given by the poles of the level density), but if one is interested only in the *coarse-grained* level density. For this, we define a smoothed quantum-mechanical level density by a convolution of (1) with a normalized Gaussian:

$$g_\gamma(E) = \frac{1}{\sqrt{\pi}\gamma} \sum_k \mathrm{e}^{-[(E-E_k)/\gamma]^2}. \tag{6}$$

Here γ is a measure of the desired energy resolution. Applying the convolution to the right-hand side of (3) will, for small enough γ, not affect the smooth part $\widetilde{g}(E)$. The convolution of the oscillating part, applied to the semiclassical trace formula (4) and evaluating the integration as usual in the stationary-phase approximation, leads to the the *coarse-grained trace formula* [7, 27]

$$\delta g_{sc}(E) = \sum_{po} \mathrm{e}^{-(\gamma T_{po}/2\hbar)^2} \mathcal{A}_{po}(E) \cos\left(\frac{1}{\hbar} S_{po}(E) - \frac{\pi}{2}\sigma_{po}\right). \tag{7}$$

The only difference to (4) is the additional exponential factor which suppresses the contributions from orbits with longer periods. Due to this factor, the periodic orbit sum now converges for not too small values of γ. Our choice of the Gaussian function in (6) is rather arbitrary; cf [20] where the regularization of the trace formula is discussed in terms of a general smooth test function. Balian and Bloch [6] have used a small imaginary part of the energy, which corresponds to using a Lorentzian smoothing function. In many physical systems, experimentally observable quantum oscillations could be well approximated through such coarse-grained trace formulae in terms of only a few short periodic orbits (see [15, 16] for examples).

3. Periodic orbit theory with spin degrees of freedom

In our present study, we want to apply the POT to systems of fermions with spin $s = 1/2$, in which the spin degrees of freedom are involved through an explicit spin dependence of the Hamiltonian. We write it as

$$\widehat{H} = \widehat{H}_0 \mathbb{1} + \widehat{H}_1 \qquad \widehat{H}_0 = \frac{\hat{\boldsymbol{p}}^2}{2m} + V(\boldsymbol{r}) \tag{8}$$

and assume the spin-dependent part to have the following general form of a spin–orbit interaction:

$$\widehat{H}_1 = \hbar\kappa \widehat{\boldsymbol{C}}(\boldsymbol{r}, \hat{\boldsymbol{p}}) \cdot \boldsymbol{\sigma}. \tag{9}$$

Here $\boldsymbol{\sigma} = (\sigma_x, \sigma_y, \sigma_z)$ is the vector built of the three Pauli matrices and $\mathbb{1}$ is the unit 2×2 matrix acting in the spin space spanned by the Pauli spinors. The Planck constant $\hbar$ in (9) comes from the spin operator $\hat{\boldsymbol{s}} = \frac{1}{2}\hbar\boldsymbol{\sigma}$. The constant κ is such that the spin–orbit term has the correct dimension of an energy; it is composed of natural (or material) constants but does not contain $\hbar$. The vector $\boldsymbol{C}(\boldsymbol{r}, \boldsymbol{p})$, which is the phase-space symbol of the operator $\widehat{\boldsymbol{C}}(\boldsymbol{r}, \hat{\boldsymbol{p}})$, may be interpreted as an internal magnetic field with arbitrary dependence on the classical phase-space variables $\boldsymbol{r}, \boldsymbol{p}$. In the standard non-relativistic reduction of the Dirac equation, $\widehat{\boldsymbol{C}}(\boldsymbol{r}, \hat{\boldsymbol{p}})$ becomes

$$\widehat{\boldsymbol{C}}(\boldsymbol{r}, \hat{\boldsymbol{p}}) = [\boldsymbol{\nabla} V(\boldsymbol{r}) \times \hat{\boldsymbol{p}}] \tag{10}$$

with $\kappa = 1/4m^2c^2$; $V(\boldsymbol{r})$ is an external electrostatic potential. For the spherical Coulomb potential, (9) and (10) yield the Thomas term (corrected by a factor 2) well known in atomic physics.

It is by no means trivial, now, to define a classical Hamiltonian corresponding to (8), since there is no direct classical analogue of the spin. Whereas numerous attempts have been made over the last seven decades or so to describe the spin classically or semiclassically, only two approaches have lent themselves to an inclusion of spin degrees of freedom in semiclassical trace formulae. These are the approaches developed by Littlejohn and Flynn [17, 18], with extensions by Frisk and Guhr [19], and of Bolte and Keppeler [20]. We refer to these original papers for all details, as well as for exhaustive references to the earlier literature. Here we shall briefly present the resulting formulae which will be applied and tested for various model systems in the following sections.

Bolte and Keppeler [20] started from the Dirac Hamiltonian to derive a relativistic trace formula which, to our knowledge, has not yet been applied to physical systems. They also started from the non-relativistic Pauli equation for a charged particle with spin $1/2$ in an external magnetic field $\boldsymbol{B}(\boldsymbol{r})$, for which we have

$$\widehat{H}_0 = \frac{1}{2m}\left[\hat{\boldsymbol{p}} - \frac{e}{c}\boldsymbol{A}(\boldsymbol{r})\right]^2 + V(\boldsymbol{r}) \qquad \widehat{H}_1 = -\frac{e\hbar}{2mc}\boldsymbol{B}(\boldsymbol{r})\cdot\boldsymbol{\sigma}. \tag{11}$$

Using the same techniques as in the derivation of their relativistic trace formula, they discuss two limits for introducing the semiclassical approximation. The Zeeman term $\widehat{H}_1$ in (11) is not a spin–orbit interaction, but Bolte and Keppeler [20] argue that the extension of their methods to the more general form (9) is straightforward. We therefore present their approach below for the general spin–orbit Hamiltonian (9).

3.1. Weak-coupling limit

In the 'weak-coupling' limit (WCL), the semiclassical approximation is systematically performed by the usual expansion in powers of $\hbar$. Because of the explicit appearance of $\hbar$ in $\widehat{H}_1$, the limit $\hbar \to 0$ leads to the classical Hamiltonian $H_{cl}(\boldsymbol{r},\boldsymbol{p}) = H_0(\boldsymbol{r},\boldsymbol{p})$ whose periodic orbits enter the trace formula. The spin degrees of freedom here are not coupled to the classical motion. Their contribution to the trace formula enters through the trace of a 2×2 matrix $\mathsf{d}(t)$ which obeys the 'spin transport equation'

$$\frac{\mathrm{d}}{\mathrm{d}t}\,\mathsf{d}(t) = -\mathrm{i}\kappa[\boldsymbol{C}(\boldsymbol{r},\boldsymbol{p})\cdot\boldsymbol{\sigma}]\,\mathsf{d}(t) \qquad \mathsf{d}(0) = \mathbb{1} \tag{12}$$

to be evaluated along each periodic orbit $\boldsymbol{r}_{po}(t)$, $\boldsymbol{p}_{po}(t)$ found from $H_0(\boldsymbol{r},\boldsymbol{p})$. This equation describes the spin precession about the instantaneous internal magnetic field $\boldsymbol{C}(\boldsymbol{r},\boldsymbol{p})$ along the periodic orbit. Using the solution of (12) for each orbit, the trace formula is given, to leading order in $\hbar$, by [20]

$$\delta g_{sc}(E) = \sum_{po} \mathcal{A}_{po}(E)\,\mathrm{tr}\,\mathsf{d}(T_{po})\cos\left(\frac{1}{\hbar}S_{po}(E) - \frac{\pi}{2}\sigma_{po}\right) \tag{13}$$

where $T_{po} = \mathrm{d}S_{po}(E)/\mathrm{d}E$ is the period of each (repeated) orbit. Since the periodic orbits are not affected by the spin motion, the only difference to the standard trace formula (4) is the appearance of the spin modulation factor $\mathrm{tr}\,\mathsf{d}(T_{po})$; all other ingredients are evaluated in the usual manner for the unperturbed periodic orbits of H_0. One may therefore consider this treatment as an adiabatic limit of fast spin motion and slow spatial motion $\boldsymbol{r}(t)$, but Bolte and Keppeler [20] argue that this adiabatic assumption is not needed for formula (13) to be true to leading order in $\hbar$.

Through the factor $\mathrm{tr}\,\mathsf{d}(T_{po})$ the contribution of a given periodic orbit depends on the overlap of the spin directions at the beginning and the end of its period. An orbit for which these two directions are identical has simply $\mathrm{tr}\,\mathsf{d}(T_{po}) = 2$, whereas an orbit for which these directions are antiparallel does not contribute at all to the trace formula (13).

For self-retracing orbits, i.e. librations between two turning points in coordinate space, the spin precession described by (12) is reversed at each turning point, and hence the spin direction is brought back to its initial value after a full period. Such orbits therefore only acquire a trivial factor $\mathrm{tr}\,\mathsf{d}(T_{po}) = 2$ compared to the trace formula (4). For systems which possess only self-retracing periodic orbits (see, e.g., the examples in sections 5 and 6), formula (13) thus reduces to the trivial recipe of incorporating the spin by a simple degeneracy factor 2 in the level density, which cannot account for the spin–orbit interaction effects.

3.2. Strong-coupling limit

To obtain the 'strong-coupling' limit (SCL), Bolte and Keppeler [20] follow the philosophy of [18, 19] by absorbing the Planck constant $\hbar$ in (11) into the Bohr magneton $\mu = e\hbar/2mc$, thus considering μ as a constant in the semiclassical limit $\hbar \to 0$. Similarly, for the spin–orbit Hamiltonian (9) one absorbs $\hbar$ into the constant $\bar{\kappa} = \hbar\kappa$. The fact that this corresponds to a double limit $\hbar \to 0$ and $\kappa \to \infty$, with $\bar{\kappa} = \hbar\kappa$ kept constant, justifies the name 'strong-coupling' limit.

The symbol of the full Hamiltonian in phase space now remains a 2×2 matrix which after diagonalization leads to the two classical Hamiltonians

$$H_{\pm}(\boldsymbol{r}, \boldsymbol{p}) = H_0(\boldsymbol{r}, \boldsymbol{p}) \pm \bar{\kappa}|\boldsymbol{C}(\boldsymbol{r}, \boldsymbol{p})| \tag{14}$$

which can be considered as two adiabatic Hamiltonians with opposite spin polarizations. They create two classes of dynamics, whose periodic orbits must be superposed in the final trace formula. Such a trace formula has, however, not been derived explicitly so far. Littlejohn and Flynn [17] argued that a non-canonical transformation of the phase-space variables $\boldsymbol{r}, \boldsymbol{p}$ would be necessary to calculate the amplitudes. Frisk and Guhr [19] surmised, based upon Fourier transforms of quantum spectra, that this is not necessary, provided that the actions $S^{\pm}_{po}$ of the periodic orbits generated by the Hamiltonians $H_{\pm}$ be corrected by some phases accumulated along the periodic orbits:

$$\frac{1}{\hbar}S^{\pm}_{po} \to \frac{1}{\hbar}S^{\pm}_{po} + \Delta\Phi_{\pm} \qquad \Delta\Phi_{\pm} = \oint_{po} \left(\lambda^{\mathrm{B}}_{\pm} + \lambda^{\mathrm{NN}}_{\pm}\right) \mathrm{d}t. \tag{15}$$

The phase velocities $\lambda^{\mathrm{B}}_{\pm}, \lambda^{\mathrm{NN}}_{\pm}$, which have been called the 'Berry' and the 'no-name' terms [17, 18], arise as first-order $\hbar$ corrections in the semiclassical expansion of the symbol of the Hamiltonian matrix. Bolte and Keppeler [20] have used their techniques to give this prescription a rigorous justification. For the Hamiltonians (14) with (10), the above phase velocities can be calculated most easily in terms of the polar angles θ, ϕ defining the unit vector of the instantaneous direction of $\boldsymbol{C}(\boldsymbol{r}, \boldsymbol{p})$, i.e., $\boldsymbol{e}_C = (\cos\phi\sin\theta, \sin\phi\sin\theta, \cos\theta)$, and of the Hesse matrix of the potential, $\mathtt{V}''_{ij} = \partial^2 V(\boldsymbol{r})/\partial r_i \partial r_j$ $(i, j = x, y, z)$, evaluated along the periodic orbits, and are given by [19]

$$\lambda^{\mathrm{B}}_{\pm} = \mp\frac{1}{2}(1 - \cos\theta)\dot{\phi} \qquad \lambda^{\mathrm{NN}}_{\pm} = -\frac{\bar{\kappa}}{2}\boldsymbol{e}_C^T \mathtt{V}'' \boldsymbol{e}_C. \tag{16}$$

Clearly, in the SCL the spin affects the classical dynamics, albeit only in an adiabatic, polarized fashion. Moreover, there is a serious limitation to the procedure outlined above. Whenever $\boldsymbol{C} = \boldsymbol{0}$ at a given point in (or in a subspace of) phase space, the two Hamiltonians $H_{\pm}$ become degenerate and singularities arise, both in the classical equations of motion and

in the calculation of the phase corrections (16) and the stabilities of the periodic orbits. Such points are called 'mode conversion' (MC) points. A similar situation occurs in the chemistry of molecular reactions when two or more adiabatic surfaces intersect. The MC poses a difficult problem in semiclassical physics and chemistry that has not been satisfactorily solved so far for systems with more than one spatial dimension (see [28] for a discussion of the MC in one dimension).

For self-retracing periodic orbits, all components of the momentum $\boldsymbol{p}$ are zero at the turning points. Hence, a spin–orbit interaction of the standard Thomas type (10) will, in the SCL, lead to MC at the turning points. In this case, both the WCL and the SCL break down, and an improved treatment becomes necessary to include such orbits in a semiclassical trace formula. A new approach that is free of the MC problem has just been proposed [29]; its results will be presented in a forthcoming paper.

4. Two-dimensional electron systems with Rashba term

In this section we shall investigate a two-dimensional electron gas (2DEG) with a spin–orbit interaction of the Rashba type [30]. We will also include an external magnetic field and an external potential $V(\boldsymbol{r}) = V(r_x, r_y)$ which causes a lateral confinement of the 2DEG (see, e.g., [31]). The Rashba term can be written in the form

$$\widehat{H}_1 = \hbar\kappa\widehat{\boldsymbol{C}}(\boldsymbol{r},\hat{\boldsymbol{p}})\cdot\hat{\boldsymbol{\sigma}} \qquad \widehat{\boldsymbol{C}}(\boldsymbol{r},\hat{\boldsymbol{p}}) = \begin{pmatrix} -\langle v_z'\rangle\hat{p}_y \\ \langle v_z'\rangle\hat{p}_x \\ \hat{p}_y\partial V(\boldsymbol{r})/\partial r_x - \hat{p}_x\partial V(\boldsymbol{r})/\partial r_y \end{pmatrix}. \tag{17}$$

Here $\langle v_z'\rangle$ is the mean gradient of the electrostatic potential in the z direction that confines the electron gas to the (x, y) plane, so that $z = p_z = 0$, and the constant κ depends on the band structure of the semiconductor in which the 2DEG is confined [31]. Note that the Rashba term (17) is of the standard form (10).

In section 4.1 we shall study the case of the free 2DEG for $V(\boldsymbol{r}) = 0$ in an external perpendicular homogeneous magnetic field, for which a quantum-mechanically exact trace formula is easily derived. We shall see that the WCL approach yields an analytical semiclassical trace formula which is exact only to leading order in $\hbar\kappa$ and in the limit $\kappa \to 0$. The SCL approach, however, for which we also obtain an analytical result, is demonstrated to fail for $\kappa \to 0$, but to include correctly the higher order terms in $\hbar\kappa$, and become exact in the strong-coupling limit. In section 4.2, we add an anisotropic harmonic confinement potential $V(\boldsymbol{r})$ to this system, where the WCL can be applied successfully in numerical calculations. When the external magnetic field is switched off, the remaining system has only self-retracing orbits for which both the WCL and the SCL fail. The MC problem arising in the SCL for this system will be discussed in section 6.

4.1. Free 2DEG with Rashba term in an external magnetic field

We first discuss the free 2DEG with the Rashba spin–orbit interaction (17) in a homogeneous magnetic field $\boldsymbol{B} = B_0\,\boldsymbol{e}_z$. The corresponding vector potential $\boldsymbol{A}$ is included by replacing the momentum operator in the usual way: $\hat{\boldsymbol{p}} \to \hat{\boldsymbol{\pi}} = \hat{\boldsymbol{p}} - e\boldsymbol{A}/c$. The total Hamiltonian then reads

$$\hat{H} = \frac{\hat{\boldsymbol{\pi}}^2}{2m^*}\mathbb{1} + \hbar\kappa\widehat{\boldsymbol{C}}(\boldsymbol{r},\hat{\boldsymbol{\pi}})\cdot\boldsymbol{\sigma} \qquad \widehat{\boldsymbol{C}}(\boldsymbol{r},\hat{\boldsymbol{\pi}}) = \begin{pmatrix} -\langle v_z'\rangle\hat{\pi}_y \\ \langle v_z'\rangle\hat{\pi}_x \\ 0 \end{pmatrix} \tag{18}$$

where, using the symmetric gauge for $\boldsymbol{A}$, the mechanical momentum is given by

$$\hat{\boldsymbol{\pi}} = \begin{pmatrix} \hat{p}_x \\ \hat{p}_y \\ 0 \end{pmatrix} - \frac{eB_0}{2c} \begin{pmatrix} -r_y \\ r_x \\ 0 \end{pmatrix}. \tag{19}$$

Here m^* is the effective mass of the electron and e its charge. We have omitted the spin contribution to the Zeeman term which could be trivially included by adding the magnetic field to $\widehat{C}$.

The quantum-mechanical eigenvalues of the Hamiltonian (18) are known analytically [30]:

$$E_0 = \hbar\omega_c/2 \qquad E_n^{\pm} = \hbar\omega_c(n \pm \sqrt{1/4 + \hbar 2n\widetilde{\kappa}^2}) \qquad n = 1, 2, 3, \ldots. \tag{20}$$

Here $\omega_c = eB_0/m^*c$ is the cyclotron frequency and $\widetilde{\kappa} = \kappa\langle v_z'\rangle\sqrt{m^*/\omega_c}$ is a renormalized coupling constant which we have defined in such a way that the Planck constant $\hbar$ appears explicitly in all our formulae[1]. The exact level density is then given by

$$g(E) = \delta(E - E_0) + \sum_{n=1}^{\infty}[\delta(E - E_n^+) + \delta(E - E_n^-)]. \tag{21}$$

Using Poisson summation (see, e.g., [15], section 3.2.2), this result can be identically transformed to an exact quantum-mechanical trace formula. The smooth part of (21) is $\widetilde{g}(E) = 2/\hbar\omega_c$, and the oscillating part becomes

$$\delta g(E) = \frac{2}{\hbar\omega_c} \sum_{\pm} \left(1 \pm \frac{\hbar\widetilde{\kappa}^2}{\sqrt{1/4 + 2E\widetilde{\kappa}^2/\omega_c + \hbar^2\widetilde{\kappa}^4}}\right) \times \sum_{k=1}^{\infty} \cos\left[k\,2\pi\left(\frac{E}{\hbar\omega_c} + \hbar\widetilde{\kappa}^2 \pm \sqrt{1/4 + 2E\widetilde{\kappa}^2/\omega_c + \hbar^2\widetilde{\kappa}^4}\right)\right]. \tag{22}$$

We will now analyse the system semiclassically, using both the WCL approach and the SCL approach. In the weak-coupling limit, we first need the trace formula for the unperturbed system without spin–orbit coupling, corresponding to $\widehat{H}_0 = \hat{\boldsymbol{\pi}}^2/2m^*$. This is the quantized Landau level system, whose exact trace formula is that of a one-dimensional harmonical oscillator with the cyclotron frequency ω_c and reads [15] (without spin degeneracy factor)

$$\delta g^{(\kappa=0)}(E) = \frac{2}{\hbar\omega_c} \sum_{k=1}^{\infty} (-1)^k \cos\left(k\frac{2\pi E}{\hbar\omega_c}\right). \tag{23}$$

For the Rashba term in (18), the spin transport equation (12) can be solved analytically [21], and the spin modulation factor becomes

$$\operatorname{tr} \mathsf{d}(kT_{po}) = (-1)^k 2\cos\left[k\,2\pi\sqrt{1/4 + 2E\,\widetilde{\kappa}^2/\omega_c}\right]. \tag{24}$$

With (13), the complete semiclassical trace formula in the WCL can therefore be written as

$$\delta g_{sc}^{\mathrm{WCL}}(E) = \frac{2}{\hbar\omega_c} \sum_{\pm} \sum_{k=1}^{\infty} \cos\left[k\,2\pi\left(\frac{E}{\hbar\omega_c} \pm \sqrt{1/4 + 2E\,\widetilde{\kappa}^2/\omega_c}\right)\right]. \tag{25}$$

This result is not the same as that of exact quantum mechanical (22), but it contains the correct terms of leading order in $\hbar$, in accordance with the derivation of Bolte and Keppeler [20], and the correct leading-order term in $\widetilde{\kappa}^2$. The missing terms would come about by going to higher orders in the semiclassical $\hbar$ expansion. Note also that (25) becomes exact in the limit $\widetilde{\kappa} \to 0$.

[1] In the literature on the Rashba term, the constant $\alpha = \hbar^2\kappa\langle v_z'\rangle$ is frequently used, see [30, 31].

Recently, Keppeler and Winkler [32] have analysed the anomalous magnetoresistance oscillations of a quasi-2DEG in GaAs semiconductors, employing two kinds of spin–orbit interactions one of which was of the Rashba type (18). They applied the WCL trace formula (13) and obtained good agreement with quantum-mechanical results. As the spin–orbit interaction in GaAs is rather weak, we assume that their results were not sensitive to the missing higher order semiclassical terms, which explains their good agreement.

It is very instructive now to compare the above result with that of an analysis using the strong-coupling limit. The SCL Hamiltonians (14) become $H_\pm(\boldsymbol{r},\boldsymbol{p}) = H_0(\boldsymbol{r},\boldsymbol{p}) \pm \tilde{\tilde{\kappa}}\sqrt{2\omega_c H_0(\boldsymbol{r},\boldsymbol{p})}$ with $\tilde{\tilde{\kappa}} = \hbar\tilde{\kappa}$. It is easy to see that $H_0(\boldsymbol{r},\boldsymbol{p}) = E_0$ is a constant of motion. The equations of motion derived from $H_\pm$ therefore become linear, representing one-dimensional harmonic oscillators as for the Landau orbits of the unperturbed system H_0. Instead of the cyclotron frequencies ω_c they have, however, the modified eigenfrequencies

$$\omega_\pm = \omega_c(1 \pm \tilde{\tilde{\kappa}}\sqrt{\omega_c/2E_0}). \tag{26}$$

Since $\boldsymbol{C}(\boldsymbol{r},\boldsymbol{p})$ does not change its sign along the modified Landau orbits, the system does not suffer from the mode conversion problem and the SCL can be safely applied. The action integrals of the primitive orbits are simply found to be $S_\pm = 2\pi E_0/\omega_c$, as for the unperturbed system, but expressing them in terms of the conserved total energy $E = E_0 \pm \tilde{\tilde{\kappa}}\sqrt{2\omega_c E_0}$ one finds

$$S_\pm(E) = 2\pi\left(\frac{E}{\omega_c} + \tilde{\tilde{\kappa}}^2 \mp \sqrt{2E\tilde{\tilde{\kappa}}^2/\omega_c + \tilde{\tilde{\kappa}}^4}\right). \tag{27}$$

The phase velocities (16) are easily found to be $\lambda_\pm^B = \mp\dot{\phi}/2 = \pm\omega_\pm/2$ and $\lambda_\pm^{NN} = 0$, so that the overall phase correction (15) becomes $\Delta\Phi_\pm = \pm\pi$ for each repetition of the primitive orbits. Inserting these results into the trace formula of the one-dimensional harmonic oscillator, i.e., equation (23) with ω_c replaced by $\omega_\pm$, using $T_\pm = 2\pi/\omega_\pm = \mathrm{d}S_\pm/\mathrm{d}E$, and summing over both orbit types, we obtain the semiclassical trace formula in the SCL (exhibiting again the $\hbar$ contained in $\tilde{\tilde{\kappa}}$)

$$\delta g_{sc}^{\mathrm{SCL}}(E) = \frac{2}{\hbar\omega_c}\sum_\pm\left(1 \pm \frac{\hbar\tilde{\kappa}^2}{\sqrt{2E\tilde{\kappa}^2/\omega_c + \hbar^2\tilde{\kappa}^4}}\right) \times \sum_{k=1}^{\infty}\cos\left[k2\pi\left(\frac{E}{\hbar\omega_c} + \hbar\tilde{\kappa}^2 \pm \sqrt{2E\,\tilde{\kappa}^2/\omega_c + \hbar^2\tilde{\kappa}^4}\right)\right]. \tag{28}$$

It is interesting to note that hereby the Berry term, yielding the phase correction $k\Delta\Phi_\pm = \pm k\pi$, cancels the alternating sign $(-1)^k$ in (23). We note that result (28) would be exactly identical to the quantum-mechanical result (22), if it were not for the missing term $1/4$ under the roots. We see, therefore, that the SCL result will fail in the limit $\tilde{\kappa} \to 0$, since the alternating sign $(-1)^k$ arises precisely from that missing term $1/4$ in the actions. On the other hand, the SCL trace formula (28) does correctly include the higher order terms in $\hbar\tilde{\kappa}^2$, both in actions and amplitudes, becoming exact in the limit of a large spin–orbit coupling parameter $\tilde{\kappa}$, as could be hoped. Note that (28) becomes exact also in the limit of large energy E. That the SCL trace formula fails in the limit $\tilde{\kappa} \to 0$ is not surprising because of the non-analytic behaviour of the Hamiltonians 14, as already pointed out in [17].

4.2. A quantum dot with external magnetic field

We now add a lateral confining potential $V(r_x, r_y)$ to the previous system. This is a simple model for a two-dimensional quantum dot which nowadays can easily be manufactured in

semiconductor heterostructures. We choose the confining potential to be harmonic, so that the Hamiltonian becomes

$$\hat{H} = \frac{\hat{\pi}^2}{2m^*}\mathbb{1} + \frac{m^*}{2}\left(\omega_x^2 r_x^2 + \omega_y^2 r_y^2\right)\mathbb{1} + \hbar\kappa\,\widehat{C}(\boldsymbol{r}, \hat{\pi})\cdot\hat{\boldsymbol{\sigma}}. \tag{29}$$

The Rashba term $\widehat{C}$ now acquires also a z component as in (17) and reads

$$\widehat{C}(\boldsymbol{r}, \hat{\pi}) = \begin{pmatrix} -\langle v_z'\rangle\hat{\pi}_y \\ \langle v_z'\rangle\hat{\pi}_x \\ m^*\omega_x^2 r_x\hat{\pi}_y - m^*\omega_y^2 r_y\hat{\pi}_x \end{pmatrix}. \tag{30}$$

In the case where the two oscillator frequencies ω_x and ω_y are identical, the total system has axial symmetry and is integrable even including the spin–orbit term, with the eigenvalues of the total angular momentum in z direction, $\hat{J}_z = \hat{L}_z + \hat{s}_z$, being constants of the motion. An exact trace formula can then be found by the EBK quantization following the methods of [18]. We will not discuss the integrable system here and refer the interested reader to [21]. A less trivial situation arises when the frequencies ω_x and ω_y are different and the system with spin–orbit coupling is no longer integrable.

Since a realistic spin–orbit coupling in most semiconductors is weak, we shall only use the WCL here to derive a semiclassical trace formula for the Hamiltonian (29). The system without spin–orbit coupling is biquadratic in the space and momentum variables and can be transformed to become separable in its normal modes. The normal-mode frequencies are

$$\omega_\pm = \left[\frac{1}{2}\left(\omega_c^2 + \omega_x^2 + \omega_y^2 \pm \sqrt{\left(\omega_c^2 + \omega_x^2 + \omega_y^2\right)^2 - 4\omega_x^2\omega_y^2}\right)\right]^{1/2}. \tag{31}$$

The exact eigenenergies are thus given in terms of two oscillator quantum numbers n_+ and n_-:

$$E_{n_+,n_-} = \hbar\omega_+(n_+ + 1/2) + \hbar\omega_-(n_- + 1/2) \qquad n_\pm = 0, 1, 2, \ldots. \tag{32}$$

The semiclassical trace formula for such a system is known [33] and quantum-mechanically exact:

$$\delta g^{(\kappa=0)}(E) = \sum_\pm \frac{1}{\hbar\omega_\pm}\sum_{k=1}^{\infty}(-1)^k \frac{1}{\sin\left[k\pi(\omega_\mp/\omega_\pm)\right]}\sin\left(k\frac{2\pi E}{\hbar\omega_\pm}\right). \tag{33}$$

Note that this formula is only useful when ω_+/ω_- is irrational. For rational frequency ratios, careful limits must be taken to cancel all singularities, see [33] for details. However, for a finite external field $B_0 \neq 0$, the ratio ω_+/ω_- can always be made irrational by an infinitesimal change of the field strength, so that equation (33) is adequate for all practical purposes. The semiclassical origin of this trace formula is given by the existence of only two isolated rotating orbits with frequencies ω_+ and ω_-, whose shapes in coordinate space are ellipses. Each orbit contributes one of the above two sums; k is the repetition number of the primitive orbits (which have $k = 1$).

We next have to calculate the spin modulation factors by solving equation (12) along the unperturbed elliptic orbits. This could only be done numerically. It is, however, sufficient to calculate the modulation factors for the primitive orbits only. Using the property $\mathrm{tr}\,\mathsf{d}(kT_{po}) = \mathrm{tr}\,\mathsf{d}^k(T_{po})$, the final trace formula in the WCL is then given by

$$\delta g_{sc}(E) = \sum_\pm \frac{1}{\hbar\omega_\pm}\sum_{k=1}^{\infty}(-1)^k \frac{\mathrm{tr}\,\mathsf{d}^k(T_\pm)}{\sin\left[k\pi(\omega_\mp/\omega_\pm)\right]}\sin\left(k\frac{2\pi E}{\hbar\omega_\pm}\right) \tag{34}$$

where $T_\pm = 2\pi/\omega_\pm$ are the periods of the unperturbed primitive orbits.

In figure 1 we compare the results for the oscillating parts $\delta g(E)$ of the coarse-grained level density for $\gamma = 0.3\,\hbar\omega_0$; all energies are in units of $\hbar\omega_0$. The deformation of the confinement

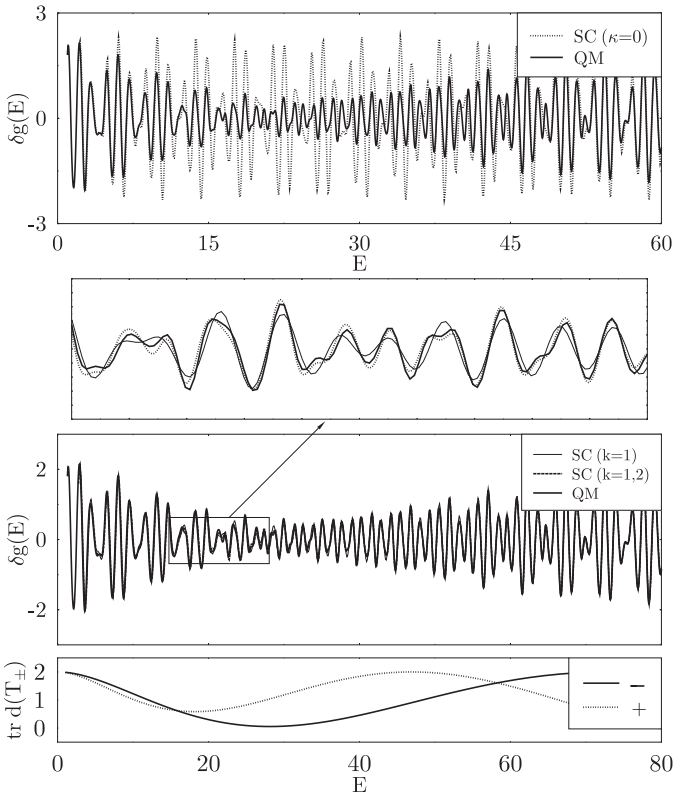

Figure 1. Upper three panels: coarse-grained (with $\gamma = 0.3\hbar\omega_0$) oscillating part $\delta g(E)$ of level density of the two-dimensional quantum dot with Rashba term (energy units: $\hbar\omega_0$). Heavy solid lines: full quantum results (QM) including Rashba term. Dotted line in the top panel: trace formula (33) for $\kappa = 0$. Solid and dashed lines in second and third panels: semiclassical trace formula (34) (SC) with only first ($k = 1$) and up to second harmonics ($k = 2$) included. Lowest panel: spin modulation factors $\mathrm{tr}\,\mathsf{d}(T_+)$ and $\mathrm{tr}\,\mathsf{d}(T_-)$.

potential was fixed by $\omega_x = \omega_0$ and $\omega_y = 1.23\,\omega_0$, and the cyclotron frequency was chosen to be $\omega_c = 0.2\,\omega_0$. In our numerical calculations we have set $\hbar = \omega_0 = m^* = e = c = \langle v_z' \rangle = 1$. In these units, the spin–orbit coupling parameter was chosen to be $\kappa = 0.1$. The heavy solid lines in the upper three panels represent the full quantum-mechanical result obtained from an exact diagonalization of the Hamiltonian (29) on the basis of $\widetilde{H}_0$. In the top panel, the semiclassical trace formula (33) without spin–orbit interaction is shown (only $k = 1$ and $k = 2$ contribute visibly). It clearly demonstrates that the effect of the spin–orbit interaction on the level density, even at this resolution, is dramatic. In the next two panels, the spin–orbit interaction has been included in the semiclassical WCL trace formula (34), using the numerical spin modulation factors. We see that the agreement is improved radically, especially if the second repetitions ($k = 2$) are added. The difference between quantum mechanics (QM) and semiclassics (SC) can clearly be seen only in the close-up (second panel), which selects the energy region $11 \lesssim E/(\hbar\omega_0) \lesssim 21$, where the disagreement actually is worst. The bottom panel shows the energy dependence of the two spin modulation factors $\mathrm{tr}\,\mathsf{d}(T_+)$ and $\mathrm{tr}\,\mathsf{d}(T_-)$ of the primitive orbits. Clearly, the strong long-range modulation in the amplitude of $\delta g(E)$ is the result of the spin–orbit interaction; it is correctly reproduced in the WCL approach through the inclusion of the spin modulation factors.

This concludes the discussion of the system with magnetic field $B_0 \neq 0$. We note at this point that the case $B_0 = 0$ with irrational frequency ratio ω_x/ω_y is not accessible in the WCL. This follows from the fact that in the system without spin–orbit coupling, the only periodic orbits are the self-retracing librations along the principal axes. As already discussed at the end of section 3.1, the WCL fails here in that it gives only the trivial modulation factor $\mathrm{tr}\,\mathtt{d}(T_{po}) = 2$ for both the orbits. On the other hand, the SCL suffers from the MC problem. We will discuss this problem explicitly in section 6, where we return to the above system with $B_0 = 0$.

5. Three-dimensional harmonic oscillator with standard spin–orbit interaction

We now discuss a three-dimensional system with a spin–orbit interaction of the Thomas type, as is well known from non-relativistic atomic and nuclear physics. In order to perform as many calculations as possible analytically, we choose again a harmonic-oscillator potential for $V(\boldsymbol{r})$. This potential is not only the prototype for any system oscillating harmonically around its ground state, but also has actually been used in nuclear physics as a realistic shell model[2] for light nuclei [23], provided that the spin–orbit interaction was included with the correct sign [24].

We thus start from the following Hamiltonian:

$$\widehat{H} = \widehat{H}_0 \mathbb{1} + \hbar\kappa\, \hat{\boldsymbol{C}}(\boldsymbol{r}, \hat{\boldsymbol{p}}) \cdot \hat{\boldsymbol{\sigma}} \qquad \hat{\boldsymbol{C}}(\boldsymbol{r}, \hat{\boldsymbol{p}}) = \nabla V(\boldsymbol{r}) \times \hat{\boldsymbol{p}} \tag{35}$$

with

$$\widehat{H}_0 = \frac{1}{2}\hat{\boldsymbol{p}}^2 + V(\boldsymbol{r}) \qquad V(\boldsymbol{r}) = \sum_{i=x,y,z} \frac{1}{2}\omega_i^2 r_i^2. \tag{36}$$

Here $\boldsymbol{r} = (r_x, r_y, r_z)$ and $\boldsymbol{p} = (p_x, p_y, p_z)$ are three-dimensional vectors. We express the three oscillator frequencies in terms of two deformation parameters α, β:

$$\omega_x = \omega_0 \qquad \omega_y = (1+\alpha)\omega_0 \qquad \omega_z = (1+\alpha)^\beta \omega_0. \tag{37}$$

and use $\hbar\omega_0$ as energy units. For $\alpha = 0$, $\beta = 1$ the system has spherical symmetry, for $\beta = 1$ and $\alpha \neq 0$ it has only axial symmetry. κ will be measured in units of $(\hbar\omega_0)^{-1}$.

We shall first (section 5.1) briefly discuss the quantum-mechanical spectrum of the system, and then (section 5.2) investigate it in more detail by the semiclassical methods. The most interesting case is that where the oscillator frequencies are mutually irrational, so that the unperturbed classical Hamiltonian H_0 has only self-retracing periodic orbits. In this case the WCL cannot handle the spin–orbit coupling, and we must resort to the SCL. As we will show, the leading periodic orbits with shortest periods in this case do not undergo mode conversion. We therefore use this system for a representative case study, for which a trace formula can be successfully derived (cf [22, 21]) within the SCL.

5.1. Quantum-mechanical spectrum

In general, the system (35) is not integrable. There are, however, two well-known integrable cases for which the quantum spectrum is analytically known: the separable system (36) without coupling ($\kappa = 0$) and the spherical system ($\alpha = 0$) including coupling. The unperturbed harmonic oscillator has the spectrum

$$E_{n_x n_y n_z} = \sum_{i=x,y,z} \hbar\omega_i (n_i + 1/2) \qquad n_i = 0, 1, 2, \ldots. \tag{38}$$

[2] The angular momentum dependent $\hat{L}^2$ term included in the Nilsson model [23] is of minor importance in light nuclei; it is left out here to simplify our investigation.

The spherical system ($\alpha = 0$) with coupling $\kappa \neq 0$, for which $\hat{\boldsymbol{C}}(\boldsymbol{r}, \hat{\boldsymbol{p}}) = \omega_0^2 \hat{\boldsymbol{L}}$, has the spectrum

$$E_{nlj} = \hbar\omega_0(2n + l + 3/2) + \kappa(\hbar\omega_0)^2 \times \begin{cases} l & \text{for} \quad j = l + 1/2 \\ -(l+1) & \text{for} \quad j = l - 1/2 \end{cases} \tag{39}$$

where $n, l = 0, 1, 2, \ldots$ and $j = l \pm 1/2$ is the total angular momentum. The spin–orbit term is only to be included for $l > 0$. Each level E_{nlj} has the usual angular momentum degeneracy $(2j + 1)$ which equals 2 for $l = 0$. Note that in nuclear physics, κ is negative [23, 24].

The non-integrable cases require numerical methods for determining the energy spectrum. Here we used the diagonalization in the basis $\mathrm{i}^{n_y}|n_x, n_y, n_z, s_z\rangle$ of the unperturbed Hamiltonian $\widehat{H}_0$ (36) with the eigenenergies (38), where $|s_z\rangle$ with $s_z = \pm 1$ are the spin eigenstates of $\hat{\sigma}_z$. The inclusion of the phase i^{n_y} leads to real matrix elements; furthermore, the conservation of the signatures $(-1)^{n_x+n_y+n_z}$ and $(-1)^{n_x+n_y}s_z$ allows one to separate the Hamiltonian matrix into smaller uncoupled blocks (see [34] for details).

5.2. Semiclassical analysis

5.2.1. Smooth level density. When one wants to compare results of semiclassical trace formulae with quantum-mechanical level densities, one has to subtract from the latter the smooth part $\widetilde{g}(E)$ (see section 2). For the Hamiltonian (35), $\widetilde{g}(E)$ can be calculated analytically within the extended Thomas–Fermi (TF) method, which has already been done long ago [35]. The result, as an expansion both in $\hbar$ and powers of κ, reads

$$\begin{aligned} \widetilde{g}(E) = {} & \frac{E^2}{\hbar^3\omega_x\omega_y\omega_z}\left\{1 + \hbar^2\kappa^2\left(\omega_x^2 + \omega_y^2 + \omega_z^2\right) + \mathcal{O}(\hbar^4\kappa^4)\right\} \\ & + \frac{2E}{3\hbar^2\omega_x\omega_y\omega_z}\left\{\hbar^3\kappa^3\left(\omega_x^2\omega_y^2 + \omega_y^2\omega_z^2 + \omega_z^2\omega_x^2\right) + \mathcal{O}(\hbar^5\kappa^5)\right\} - \frac{\left(\omega_x^2 + \omega_y^2 + \omega_z^2\right)}{12\hbar\omega_x\omega_y\omega_z} \\ & \times \left\{1 + \hbar^2\kappa^2\frac{\left(\omega_x^2 + \omega_y^2 + \omega_z^2\right)^2 + 2\left(\omega_x^2\omega_y^2 + \omega_y^2\omega_z^2 + \omega_z^2\omega_x^2\right)}{\left(\omega_x^2 + \omega_y^2 + \omega_z^2\right)} + \mathcal{O}(\hbar^4\kappa^4)\right\}. \end{aligned} \tag{40}$$

In the literature, the smooth part is often assumed to be given by the TF model. This leads, however, only to the leading term proportional to E^2. For an accurate determination of $\widetilde{g}(E)$, the leading $\hbar$ and $\hbar^2$ corrections relative to the TF term may not be neglected.

5.2.2. Trace formulae for the integrable cases. The exact spectra of the integrable cases offer again the possibility to derive trace formulae that are exact in all orders of $\hbar$. For the unperturbed harmonic oscillators, these are known [15, 33] and need not be repeated here. For the spherical case with spin–orbit interaction, the methods of [15, 33, 35] lead to the following result:

$$\begin{aligned} \delta g(E) = {} & \frac{E}{(\hbar\omega_0)^2}\sum_{\pm}\sum_{k=1}^{\infty}\frac{1}{(1 \mp \kappa\hbar\omega_0)^2}\frac{1}{\sin\left[2k\pi/(1 \mp \kappa\hbar\omega_0)\right]}\sin\left(k\frac{ET_{\pm}}{\hbar} - \frac{\pi}{2}k\sigma_{\pm}\right) \\ & + \frac{1}{\hbar\omega_0}\sum_{\pm}\sum_{k=1}^{\infty}\frac{(\mp 1 + 2\kappa\hbar\omega_0)}{2(1 \mp \kappa\hbar\omega_0)^2}\frac{1}{\sin\left[2k\pi/(1 \mp \kappa\hbar\omega_0)\right]}\sin\left(k\frac{ET_{\pm}}{\hbar} - \frac{\pi}{2}k\sigma_{\pm}\right) \\ & + \frac{1}{\hbar\omega_0}\sum_{\pm}\sum_{k=1}^{\infty}\frac{1}{(1 \mp \kappa\hbar\omega_0)^2}\frac{\cos\left[2k\pi/(1 \mp \kappa\hbar\omega_0)\right]}{\sin^2\left[2k\pi/(1 \mp \kappa\hbar\omega_0)\right]}\cos\left(k\frac{ET_{\pm}}{\hbar} - \frac{\pi}{2}k\sigma_{\pm}\right) \\ & + \frac{1}{\hbar\omega_0}\sum_{k=1}^{\infty}\frac{(-1)^{k+1}}{2\sin^2\left(k\pi\kappa\hbar\omega_0\right)}\cos\left(k\frac{ET_0}{\hbar} - \frac{\pi}{2}k\sigma_0\right) \end{aligned} \tag{41}$$

where the three periods $T_\pm$ and T_0 are given by

$$T_\pm = \frac{2\pi}{\omega_0(1 \mp \kappa\hbar\omega_0)} \qquad T_0 = \frac{2\pi}{\omega_0} \tag{42}$$

and the phases

$$\sigma_\pm = \frac{\mp 2}{1 \mp \kappa\hbar\omega_0} \qquad \sigma_0 = -4\kappa\hbar\omega_0 \tag{43}$$

play the role of non-integer Maslov integers. When added to the smooth part (40), equation (41) reproduces the exact quantum spectrum (39). This trace formula thus serves us as a test limit of the semiclassical results derived below in the non-integrable deformed cases. In T_0 we recognize the period of the classical orbits of the unperturbed Hamiltonian; the shifted periods $T_\pm$ have to be explained by the periodic orbits of the perturbed system.

In the limit $\kappa \to 0$, the sum of the smooth term (40) with $\omega_x = \omega_y = \omega_z = \omega_0$ and the oscillating term (41) yields the exact trace formula of the isotropic three-dimensional harmonic oscillator [15, 33] (which here includes the spin degeneracy factor 2)

$$g(E) = \frac{1}{(\hbar\omega_0)^3}\left[E^2 - \frac{1}{4}(\hbar\omega_0)^2\right]\left\{1 + 2\sum_{k=1}^{\infty}(-1)^k \cos\left(k\frac{2\pi E}{\hbar\omega_0}\right)\right\}. \tag{44}$$

5.2.3. Fourier transforms. Since we have no explicit quantum spectra of the perturbed system and therefore cannot derive an exact trace formula, we resort to the method of Fourier transforms of the quantum spectrum [36] in order to extract information on the periods of the system. The Hamiltonian (35) has the scaling property

$$\hat{H}(\eta\boldsymbol{r}, \eta\hat{\boldsymbol{p}}) = \eta^2\hat{H}(\boldsymbol{r}, \hat{\boldsymbol{p}}). \tag{45}$$

We see below that this scaling property holds also in the classical limit if the SCL is used. As a consequence, the energy dependence of the classical dynamics and thus of the periodic orbits is simply given by a scaling, and their actions go as $S_{po}(E) = T_{po}E$, whereby the periods $T_{po} = 2\pi/\omega_{po}$ are energy independent (but depend on κ). Therefore, the peaks in the Fourier transforms of $\delta g(E)$ with respect to the variable E will give us directly the periods T_{po} in the time domain, whereby the peak heights are given by the semiclassical amplitudes $\mathcal{A}_{po}$ and their signs give information on the relative Maslov indices.

In figure 2 we present a series of Fourier transforms of $\delta g(E)$ obtained from the numerically diagonalized quantum spectra with a coarse-graining parameter $\gamma = 0.5\hbar\omega_0$. Here the squares of the Fourier amplitudes in the time domain, plotted for different spin–orbit coupling strengths κ are shown. A slightly anisotropic ratio of frequencies $\omega_x = \omega_0$, $\omega_y = 1.1215\,\omega_0$, $\omega_z = 1.2528\,\omega_0$ was chosen. For $\kappa = 0$, the system then has only the three isolated librating orbits along the principal axes. Indeed, we see at $\kappa = 0$ the three dominant peaks with the corresponding primitive periods $T_i = 2\pi/\omega_i$ $(i = x, y, z)$. Their second harmonics $(k = 2)$ are also resolved; however, due to their larger periods they are of smaller amplitude. For $\kappa > 0$ this simple peak structure is split and ends in a completely different spectrum at $\kappa = 0.2\,(\hbar\omega_0)^{-1}$. The dotted lines are the predictions from the semiclassical SCL analysis given in the next subsection; the plots on the right-hand side indicate the shapes of the periodic orbits for increasing κ.

5.2.4. Semiclassical treatment in the SCL approach. We now analyse the system semiclassically in the SCL. According to section 3.2, the classical Hamiltonians to be used are

$$H_\pm(\boldsymbol{r}, \boldsymbol{p}) = \tfrac{1}{2}p^2 + V(\boldsymbol{r}) \pm \bar{\kappa}|\boldsymbol{C}(\boldsymbol{r}, \boldsymbol{p})| \tag{46}$$

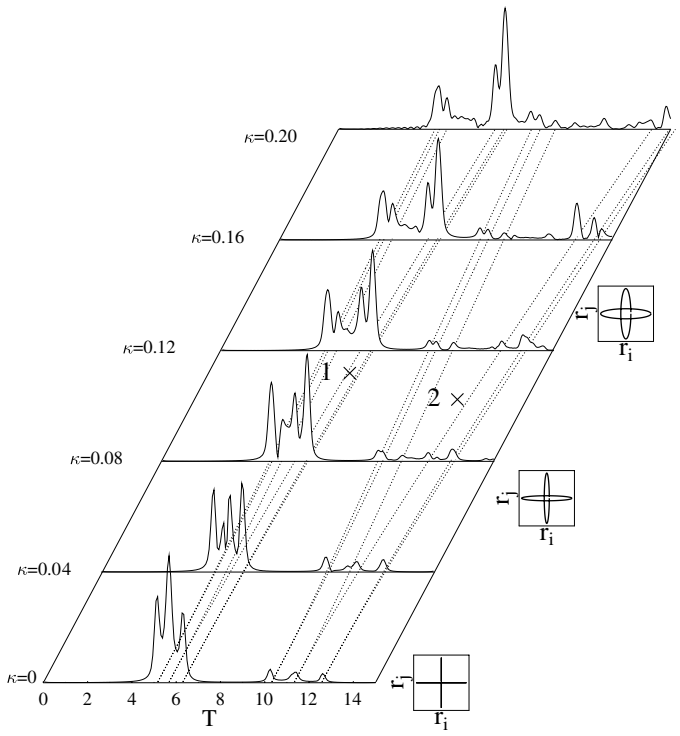

Figure 2. Fourier spectra of quantum-mechanical level density $\delta g(E)$ (coarse-grained with $\gamma = 0.5\,\hbar\omega_0$) of the three-dimensional harmonic oscillator with deformation $\alpha = 0.1212$, $\beta = 2$, and various spin–orbit strengths κ in units $(\hbar\omega_0)^{-1}$. T is in units of ω_0^{-1}. For the dotted lines and the inserts on the rhs, see figure 3.

with $\boldsymbol{C}$ given in (35) and $\bar{\kappa} = \hbar\kappa$ as discussed in section 3.2. The spin–orbit term destroys the integrability of the harmonic oscillator, but the scaling property (45) is still fulfilled. Therefore the above Fourier spectra should give us the correct periods of the periodic orbits defined by the Hamiltonians (46).

Periodic orbits. The equations of motion for the Hamiltonians (46) become

$$\begin{aligned} \dot{r}_i &= p_i \pm \epsilon_{ijk}\bar{\kappa}|\boldsymbol{C}|^{-1}\left(C_j\omega_k^2 r_k - C_k\omega_j^2 r_j\right) \\ \dot{p}_i &= -\omega_i^2 r_i \pm \epsilon_{ijk}\bar{\kappa}|\boldsymbol{C}|^{-1}\left(C_j\omega_i^2 p_k - C_k\omega_i^2 p_j\right) \qquad i, j, k \in \{x, y, z\}. \end{aligned} \tag{47}$$

This is a non-linear coupled system of six equations, and the search for periodic orbits is not easy. We have determined them numerically by a Newton–Raphson iteration employing the stability matrix [21]. Special care must be taken at the MC points where $\boldsymbol{C}(\boldsymbol{r}, \boldsymbol{p}) = 0$ and hence equations (47) are ill defined. In general, this leads to discontinuities in the shapes of the periodic orbits, due to which their stabilities cannot be defined. We shall return to the MC problem in section 6. It turns out that there exist periodic orbits which are free of MC, i.e. for which $\boldsymbol{C}(\boldsymbol{r}, \boldsymbol{p})$ never becomes zero. The existence of some particularly simple orbits follows from the fact that the three planes $r_k = p_k = 0\,(k = x, y, z)$ in phase space are invariant under the Hamiltonian flow. The coupled equations of motion for the class of two-dimensional orbits

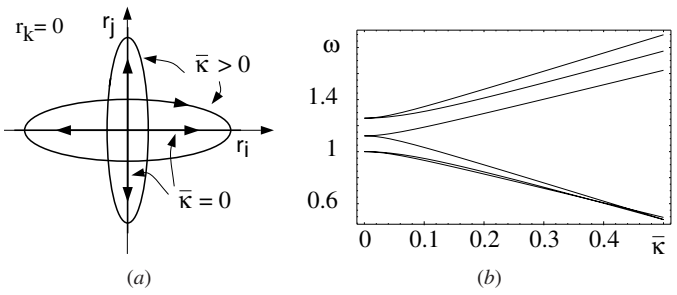

Figure 3. (*a*) The six frequencies $\omega_{ij}^{\pm}$ (50) (units: ω_0) for $ij = 12$, 23, and 31 versus $\bar{\kappa}$ (units: ω_0^{-1}). Deformations are as in figure 2. (*b*) Schematic plot of shapes of the elliptic orbits ($\bar{\kappa} > 0$) and the unperturbed librating orbits ($\bar{\kappa} = 0$) in the (i, j) plane.

lying in the (i, j) planes are

$$\begin{aligned} \dot{r}_i &= p_i \mp \epsilon_{ijk}\,\bar{\kappa}\,\mathrm{sign}(C_k)\omega_j^2 r_j \\ \dot{p}_i &= -\omega_i^2 r_i \mp \epsilon_{ijk}\,\bar{\kappa}\,\mathrm{sign}(C_k)\omega_i^2 p_j \qquad i, j, k \in \{x, y, z\} \end{aligned} \tag{48}$$

where i and j refer to the in-plane variables and k to the normal of each plane. Assuming that there exist solutions with $C_k \neq 0$, we can put $\mathrm{sign}(C_k) = 1$, since for each such orbit, there exists a time-reversed partner which belongs to the opposite of the two Hamiltonians $H_{\pm}$. Hence we obtain the system of equations

$$\begin{aligned} \dot{r}_i &= p_i \mp \epsilon_{ijk}\,\bar{\kappa}\omega_j^2 r_j \\ \dot{p}_i &= -\omega_i^2 r_i \mp \epsilon_{ijk}\,\bar{\kappa}\omega_i^2 p_j \qquad i, j, k \in \{x, y, z\} \end{aligned} \tag{49}$$

which now is strictly linear and can be solved by finding the normal modes. The solutions are two periodic orbits of ellipse form in each invariant plane (i, j). For the two Hamiltonians $H_{\pm}$ this gives altogether 12 planar periodic orbits which come in doubly degenerate pairs. We therefore find six different orbits (denoted by $\gamma_{ij}^{\pm}$ in figure 5 below) with the frequencies

$$\omega_{ij}^{\pm} = \left[\left(\omega_j^2 + \omega_i^2 + 2\bar{\kappa}^2\omega_i^2\omega_j^2 + \sqrt{\left(\omega_j^2 - \omega_i^2\right)^2 + 8\bar{\kappa}^2\omega_i^2\omega_j^2\left(\omega_i^2 + \omega_j^2\right)}\right)\right]^{1/2}. \tag{50}$$

The rhs of figure 3 shows these frequencies versus the spin–orbit coupling parameter $\bar{\kappa}$. On the lhs we illustrate the periodic orbits for $\bar{\kappa} \neq 0$ (ellipses) and the unperturbed libration orbits for $\bar{\kappa} = 0$. The periods $T_{ij}^{\pm} = 2\pi \big/ \omega_{ij}^{\pm}$ fit perfectly the positions of the most pronounced peaks in the Fourier spectra of figure 2 (cf the dotted lines there), when the appropriate deformations ω_i, ω_j are chosen. Some of the minor peaks may be attributed to non-planar orbits (see below).

In the spherical limit, the same procedure leads to a very simple analytical result. Due to the conserved angular momentum $\boldsymbol{L} = \boldsymbol{r} \times \boldsymbol{p}$, most periodic orbits are planar circles. In each plane, the equations of motion are similar to (49), with the two eigenfrequencies $\omega^{\pm}$ and corresponding periods $T^{\pm}$ given by

$$\omega^{\pm} = \omega_0(1 \pm \bar{\kappa}\omega_0) \qquad T^{\pm} = \frac{2\pi}{\omega_0(1 \pm \bar{\kappa}\omega_0)}. \tag{51}$$

The periods $T^{\pm}$ are exactly equal to the two periods $T_{\pm}$ in (42) that appear in the exact trace formula (41) of the spherical system[3]. However, the unperturbed harmonic-oscillator period

[3] Note that in the present SCL approach, the constant $\bar{\kappa}$ includes a factor $\hbar$, see section 3.2.

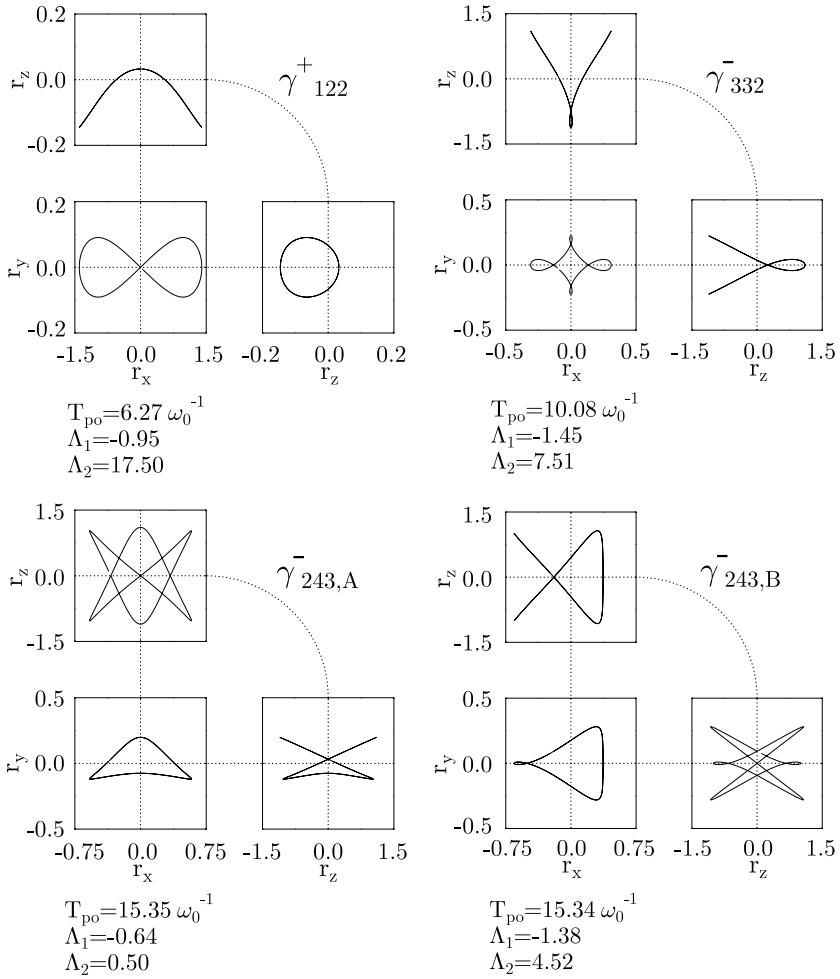

Figure 4. Shapes of four three-dimensional non-planar orbits found in the harmonic oscillator with deformations as in figure 2 and spin–orbit interaction $\bar{\kappa} = 0.2\,\omega_0^{-1}$, projected onto the three spatial planes. (See text for the periods T_{po} and stability traces Λ_1, Λ_2.)

$T_0 = 2\pi/\omega_0$ that also appears in (41) cannot be explained by the present solutions in the SCL. We surmise that it might be connected to the existence of straight-line librating orbits; these lie, however, on mode conversion surfaces and cannot be treated in the present approach. In our ongoing studies [29] where the MC problem is avoided, we can, indeed, confirm the existence of periodic orbits with the period T_0.

Besides the above harmonic planar solutions, the full non-linear system (47) leads also to non-planar three-dimensional periodic solutions with $\boldsymbol{C}(\boldsymbol{r}, \boldsymbol{p}) > 0$ (or < 0) for which mode conversion does not occur. Some of these numerically obtained orbits evaluated at $\bar{\kappa} = 0.2\,\omega_0^{-1}$ are shown in figure 4. We also give their periods T_{po} and partial traces Λ_i which determine their stabilities (see below). The orbit γ^{-}_{332} has the period $T_{po} = 10.08\,\omega_0^{-1}$ which seems to be supported numerically by a small peak seen in the uppermost Fourier spectrum of figure 2. The periods of the other orbits from figure 4 could not clearly be identified in the Fourier spectra; some of these orbits are too unstable and some of the periods lie too close to those of the leading planar orbits.

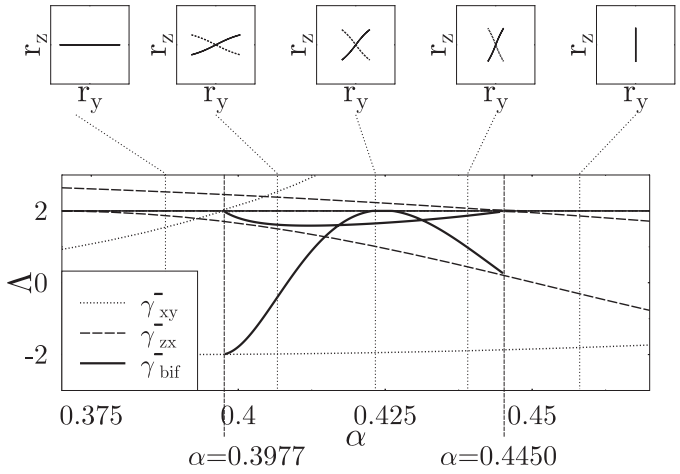

Figure 5. The bifurcation of a planar ellipse orbit under variation of the deformation parameter α. Upper panels: projection of the orbits onto the (y, z) plane. Lower panel: partial traces Λ_i of the involved orbits versus α (see text for details).

Stability amplitudes and trace formula for isolated orbits. The amplitude $\mathcal{A}_{po}$ of a periodic orbit in the trace formula is strongly dependent on its stability. For isolated orbits in a two-dimensional system, the factor $|\det(\widetilde{\mathbb{M}}_{po} - \mathbb{1})|$ in 5 equals $|2 - \operatorname{tr}\widetilde{\mathbb{M}}_{po}| = |2 - (\lambda_1 + \lambda_2)| = |2 - (\lambda_1 + 1/\lambda_1)|$, where λ_i $(i = 1, 2)$ are the eigenvalues of the stability matrix $\widetilde{\mathbb{M}}_{po}$, and thus the quantity $\operatorname{tr}\widetilde{\mathbb{M}}_{po}$ contains all information about the stability of an orbit. For a system in $d \geqslant 2$ dimensions, we can write

$$|\det(\widetilde{\mathbb{M}}_{po} - \mathbb{1})| = \prod_{i=1}^{d-1} |\Lambda_i - 2| \tag{52}$$

where the 'partial traces' Λ_i are the sums of pairs λ_i, $1/\lambda_i$ of mutually inverse eigenvalues of the $(2d-2)$-dimensional stability matrix $\widetilde{\mathbb{M}}_{po}$: $\Lambda_i = \lambda_i + 1/\lambda_i$ $(i = 1, 2, \ldots, d-1)$. An orbit is stable when $|\Lambda_i| < 2$ for all i, unstable when $|\Lambda_i| > 2$ for all i and mixed stable (or loxodromic) in all other cases. For the latter cases, the stability depends on the phase-space direction of a perturbation. Whenever $\Lambda_i = +2$ for any partial trace, a bifurcation occurs and the stability denominator (52) becomes zero. In such a situation one has to resort to uniform approximations [12, 13] in order to obtain finite semiclassical amplitudes. Non-isolated periodic orbits with $\Lambda_i = 2$ occur in degenerate families for systems with continuous symmetries and are characteristic of integrable systems; for these, the amplitudes must be obtained differently [6–9]. The symmetry breaking away from integrability can also be handled perturbatively [10] or with suitable uniform approximations [11, 14].

Most of the orbits that we have found, both planar and non-planar, undergo bifurcations when the spin–orbit parameter $\bar{\kappa}$ or the deformation parameters α, β are varied. A typical scenario is illustrated in figure 5, where α is varied at fixed $\bar{\kappa} = 0.1\,\omega_0^{-1}$ and $\beta = 2$. The partial traces Λ_i of the involved orbits are shown. One of the planar ellipse orbits (γ_{xy}^-) lying in the (x, y) plane undergoes an isochronous pitchfork bifurcation at $\alpha = 0.3977$. The new-born pair of orbits (γ_{bif}^-) is degenerate with respect to a reflection at the (x, y) plane. They are non-planar warped ellipses which rotate out of the (x, y) plane when α is increased, and then approach the (x, z) plane. Through an inverse pitchfork bifurcation at $\alpha = 0.4450$, they finally merge with another planar ellipse orbit (γ_{zx}^-) lying in the (x, z) plane. Near $\alpha \sim 0.425$, the orbit γ_{bif}^- suffers from two more bifurcations (the other orbits involved thereby are not shown).

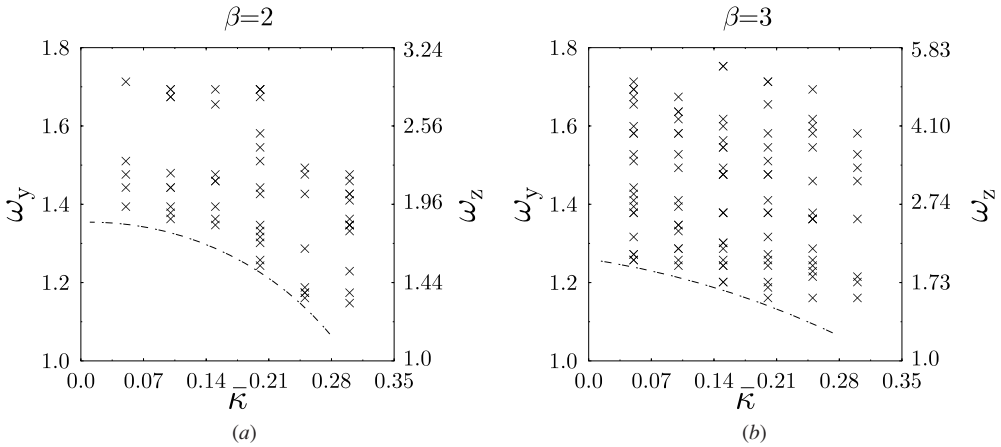

Figure 6. Bifurcations of the planar periodic orbits $\gamma_{ij}^{\pm}$ in the three-dimensional harmonic oscillator with spin–orbit interaction, given by the SCL Hamiltonians $H_{\pm}$ in (46). The crosses give the critical values of the frequencies ω_y and ω_z versus $\bar{\kappa}$ for (*a*) $\beta = 2$ and (*b*) $\beta = 3$. No bifurcations were found in the regions below the dashed lines.

This example shows that the classical dynamics of the Hamiltonians $H_{\pm}$ is mixed and quite complicated due to the unavoidable bifurcations. In principle, isolated bifurcations can be handled using the well-known uniform approximations [12, 13]. These fail, however, when two bifurcations lie so close that the difference between the corresponding actions S_{po} becomes comparable to or less than $\hbar$. It is outside the scope of the present study to attempt to regulate the Gutzwiller amplitudes by uniform approximations. In figure 6 we show by crosses the critical values of the frequencies ω_y and ω_z (in units of $\omega_x = \omega_0$) versus $\bar{\kappa}$, at which bifurcations of the planar orbits $\gamma_{ij}^{\pm}$ occur for fixed values of the deformation parameter $\beta = 2$ (figure 6(*a*)) and $\beta = 3$ (figure 6(*b*)). The other deformation parameter α is given via (37). In the deformation regions below the dashed lines, where no bifurcations occur, the semiclassical amplitudes can be used without further uniform approximation.

For the contributions of all the isolated periodic orbits away from the bifurcations, we therefore use the trace formula

$$\delta g_{\gamma}(E) = \frac{1}{\hbar\pi} \sum_{po} \mathrm{e}^{-(\gamma T_{po}/2\hbar)^2} \frac{T_{ppo}}{\sqrt{\prod_{i=1}^{d-1} |\Lambda_i - 2|}} \cos\left(\frac{1}{\hbar} S_{po} + \Delta\Phi_{po} - \frac{\pi}{2}\sigma_{po}\right) \tag{53}$$

whereby the sum po explicitly includes all periodic orbits of both Hamiltonians $H_{\pm}$. The Maslov indices σ_{po} were evaluated with the methods developed by Creagh *et al* [37], employing the recipes given in appendix D of [15]. The terms $\Delta\Phi_{po}$ are the phase corrections (15). For the planar ellipse orbits lying in the (i, j) planes, we find $\lambda_{\pm}^{B} = 0$ and $\lambda_{\pm}^{NN} = -\bar{\kappa}\omega_k^2/2$, so that $\Delta\Phi_{po} = -\bar{\kappa}\pi\omega_k^2/\omega_{ij}^{\pm}$.

In figure 7 we show the results obtained for the situation $\alpha = 0.1212, \beta = 2, \bar{\kappa} = 0.1\,\omega_0^{-1}$, for which no close-lying bifurcations exist. The quantum-mechanical coarse-grained level density $\delta g(E)$ is shown by the solid lines (QM) and includes the spin–orbit interaction in both curves (*a*) and (*b*). The semiclassical results (SC) are shown by dashed lines; in (*a*) without spin–orbit interaction, which again demonstrates that the latter dramatically changes the level density; in (*b*) with spin–orbit interaction through the trace formula (53). Only the six primitive planar orbits have been used. We see that this already leads to an excellent agreement with quantum mechanics, except at very low energies where semiclassics usually

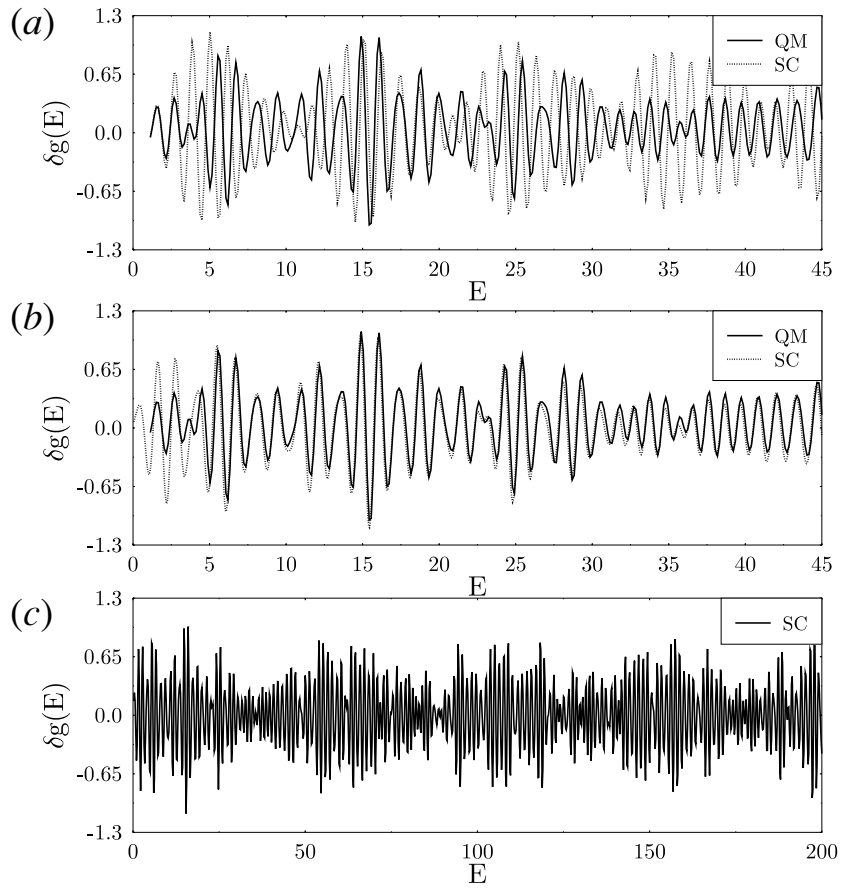

Figure 7. The coarse-grained level density $\delta g(E)$ of three-dimensional harmonic oscillator with spin–orbit interaction $\bar{\kappa} = 0.1\,\omega_0^{-1}$ (other parameters as in figure 2). Solid lines (QM) give the quantum-mechanical results with spin–orbit interaction. Dashed lines (SC) give the semiclassical results according to (53), calculated (*a*) without and (*b*) with spin–orbit interaction. (*c*) Same as SC in (*b*), but over a larger energy region.

cannot be expected to work. The curve SC in the lowest panel (*c*) shows the semiclassical result over a larger energy scale.

Similar results were obtained in the region of deformations and $\bar{\kappa}$ values below the dashed lines in figure 6, where bifurcations do not occur. In all these cases, it turned out that the inclusion of the six primitive planar orbits was sufficient within the resolution given by the coarse-graining width $\gamma = 0.5\hbar\omega_0$. This result is in agreement with the Fourier analysis of section 5.2.3 of the quantum spectra, where all dominant peaks correspond to the periods of these six orbits.

6. The problem of mode conversion

In this section we want to discuss the mode conversion (MC) problem that arises in the strong-coupling limit (SCL) following [17, 18]. In particular, we will discuss an intuitive method, suggested by Frisk and Guhr [19], to partially avoid the MC problem. This method

can qualitatively explain some of the peaks observed in the Fourier spectra of the quantum-mechanical level densities $\delta g(E)$. It can, however, not be used to calculate the amplitudes $\mathcal{A}_{po}$ required for the semiclassical trace formula.

For this purpose, we return to the 2DEG with lateral harmonic confinement discussed in section 4.2, but without external magnetic field ($B_0 = 0$). We shall again assume the oscillator frequencies ω_x and ω_y to be incommensurable (i.e. ω_x/ω_y is irrational). Then, the system without spin–orbit interaction has only the isolated self-retracing librating orbits along the axes, and the weak-coupling limit (WCL) approach of [20] cannot handle the spin–orbit interaction (except for a trivial spin factor 2 in the trace formula). We therefore have to resort to the SCL approach. In order to simplify the discussion and focus on the important points, we set $m^* = 1$ and ignore the diagonal elements of the spin–orbit interaction. We thus start from the Hamiltonian

$$\widehat{H} = \frac{1}{2}\left(\hat{p}_x^2 + \hat{p}_y^2 + \omega_x^2 r_x^2 + \omega_y^2 r_y^2\right) \mathbb{1} + \hbar\kappa \begin{pmatrix} 0 & -\hat{p}_x - \mathrm{i}\hat{p}_y \\ \hat{p}_x + \mathrm{i}\hat{p}_y & 0 \end{pmatrix} \tag{54}$$

which in the SCL leads to the classical Hamiltonians ($\bar{\kappa} = \hbar\kappa$)

$$H_\pm = \tfrac{1}{2}\left(p_x^2 + p_y^2 + \omega_x^2 r_x^2 + \omega_y^2 r_y^2\right) \pm \bar{\kappa}\sqrt{p_x^2 + p_y^2}. \tag{55}$$

Before taking the semiclassical limit, we first perform a Fourier analysis of the quantum spectrum of (54) which is easily diagonalized in the unperturbed harmonic-oscillator basis. The Hamiltonian (54) does not possess the scaling property (45) of the three-dimensional system studied in section 5. However, we can use the method of [36] by scaling the parameter $\bar{\kappa}$ away. Dividing equation (55) by $\bar{\kappa}^2$ and introducing the scaled variables $\tilde{r}_i = r_i/\bar{\kappa}$, $\tilde{p}_i = p_i/\bar{\kappa}$, we obtain the scaled Hamiltonians

$$\widetilde{H}_\pm = \tfrac{1}{2}\left(\tilde{p}_x^2 + \tilde{p}_y^2 + \omega_x^2\tilde{r}_x^2 + \omega_y^2\tilde{r}_y^2\right) \pm \sqrt{\tilde{p}_x^2 + \tilde{p}_y^2} = E/\bar{\kappa}^2 = e \tag{56}$$

so that the classical dynamics does not depend explicitly on $\bar{\kappa}$ but is determined only by the scaled energy variable e. Therefore, a Fourier transform of the quantum spectra along the path in the (E, κ) plane with constant E/κ^2 leads in the time domain to the quasiperiods $\widetilde{T}_{po}^{\pm} = s_{po}^{\pm}(e)/e$ of the periodic orbits of the Hamiltonians (56), whereby $s_{po}^{\pm}$ are their scaled actions.

In the lower part of figure 9 below we show the result of the Fourier transforms, taken at two different scaled energies. For $e = 10^5\,\hbar\omega_0/\bar{\kappa}^2$ (dashed line) only two peaks are seen. For $e = 30\,\hbar\omega_0/\bar{\kappa}^2$ (solid line), these are slightly shifted and remain the dominant peaks, whereas four additional small peaks appear (the second of these extra peaks is almost absorbed in the left dominant peak).

We now analyse the classical dynamics of the Hamiltonians (56). As in the three-dimensional system analysed in section 5.2.4, we can find orbits lying in the invariant subspaces of phase space with $\tilde{r}_i = \tilde{p}_i = 0$ for one of the degrees of freedom i (x or y). For the other degree, the one-dimensional equations of motion become

$$\dot{\tilde{r}}_i = \tilde{p}_i \pm \operatorname{sign}\tilde{p}_i \qquad \dot{\tilde{p}}_i = -\omega_i^2\tilde{r}_i. \tag{57}$$

On the axes $\tilde{p}_i = 0$ in phase space these equations are ill defined. It is still possible to solve the equations for $\tilde{p}_i \neq 0$, which leads to portions of a circle in the $(\tilde{p}_i, \tilde{r}_i)$ plane for each sign of $\tilde{p}_i$. One may then connect these partial trajectories to form periodic orbits whose shapes have, however, kinks. This is illustrated in figure 8(a). Due to the kinks, these orbits are not differentiable and their stabilities cannot be defined. Their periods can, however, be calculated analytically and become

$$T_{i,+}^{\mathrm{adia}}(e) = \frac{2}{\omega_i}\arccos\left(\frac{1-2e}{1+2e}\right) \qquad T_{i,-}^{\mathrm{adia}}(e) = \frac{4\pi}{\omega_i} - \frac{2}{\omega_i}\arccos\left(\frac{1-2e}{1+2e}\right). \tag{58}$$

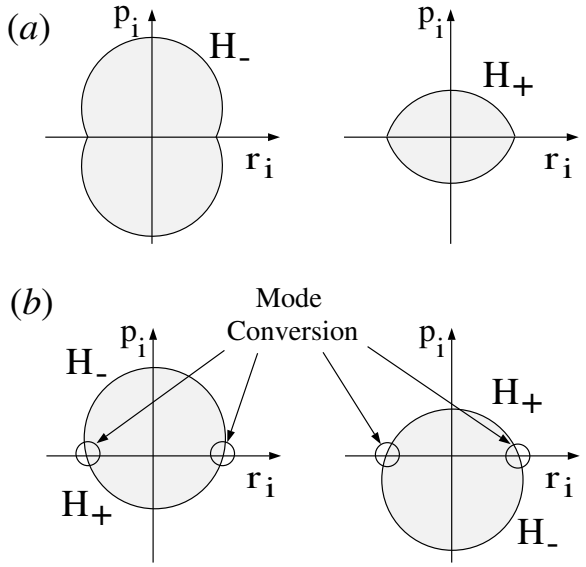

Figure 8. (*a*) Periodic orbits found from the adiabatic Hamiltonians (56). (*b*) Diabatic periodic orbits found by enforcing spin–flips $H_+ \leftrightarrow H_-$ at the mode conversion points.

From the area enclosed by the orbits, we can also obtain the scaled actions:

$$s^{\mathrm{adia}}_{i,\pm}(e) = \left(e - \frac{1}{2}\right) T^{\mathrm{adia}}_{i,\pm}(e) - \frac{2}{\omega_i}\sqrt{2e}. \tag{59}$$

We use the superscript 'adia' because the Hamiltonians $H_\pm$ correspond to the adiabatic situation where the spin polarizations are fixed.

An alternative way to use the partial solutions found from (57) has been proposed by Frisk and Guhr [19]: instead of joining the two portions obtained for both signs of $\tilde{p}_i$ on one and the same of the Hamiltonians $H_\pm$, one switches between the $H_\pm$, enforcing a spin–flip at the MC points: $H_+ \longleftrightarrow H_-$. This corresponds to the transition from the adiabatic to a diabatic basis. The orbits thus obtained are continuous circles with continuous derivatives, as illustrated in figure 8(*b*), and correspond to simple harmonic librations along the i axes. Their periods and actions are easily found to be

$$T^{\mathrm{dia}}_i = \frac{2\pi}{\omega_i} \qquad s^{\mathrm{dia}}_i(e) = \left(e + \frac{1}{2}\right)\frac{2\pi}{\omega_i}. \tag{60}$$

The superscript 'dia' indicates that we call these the diabatic orbits. Their periods are those of the Hamiltonian without spin–orbit coupling: $T^{\mathrm{dia}}_i = T^{(0)}_i = 2\pi/\omega_i$. Although their shapes are continuous and differentiable, their stabilities still cannot be calculated, because the Hessian matrices of the $H_\pm$ in phase space are singular at the MC points. In the limit $e \to \infty$, the pairs of adiabatic orbits merge into the diabatic orbits, and we get

$$T^{\mathrm{adia}}_{i,\pm}(e) \longrightarrow T^{\mathrm{dia}}_i \qquad \frac{s^{\mathrm{adia}}_{i,\pm}(e)}{e} \longrightarrow \frac{s^{\mathrm{dia}}_i(e)}{e} \longrightarrow T^{\mathrm{dia}}_i. \tag{61}$$

In the upper part of figure 9, we show the curves $s^{\mathrm{adia}}_{i,\pm}(e)/e$ by the short and long dashed lines and the curves $s^{\mathrm{dia}}_i(e)/e$ by the solid lines. We see that their values at $e = 30\hbar\omega_0/\bar{\kappa}^2$ correspond exactly to the six peaks appearing in the corresponding Fourier spectrum. The two

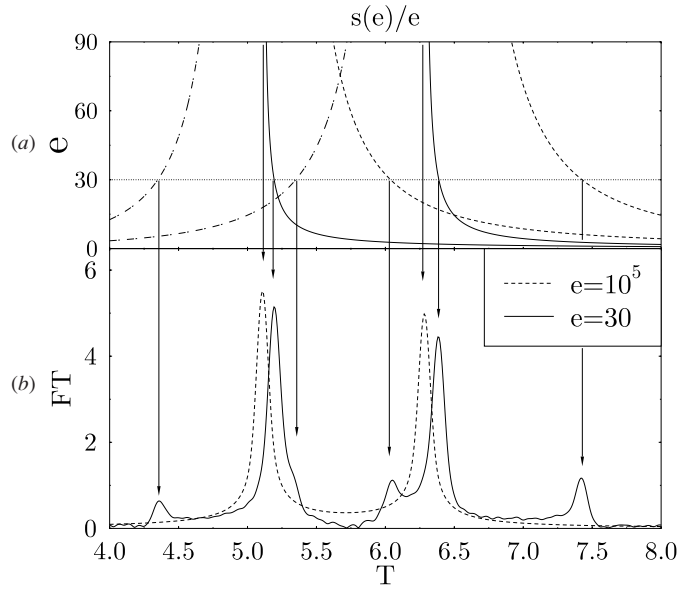

Figure 9. (*b*) Fourier spectra as in figure 2 of the quantum spectrum of the Hamiltonian (54) with $\gamma = 0.2\hbar\omega_0$, evaluated for two values of the scaled energy e (units: $\hbar\omega_0/\bar{\kappa}^2$). Deformation: $\omega_x = \omega_0$, $\omega_y = 1.23\omega_0$. (*a*) Quasiperiods $s(e)/e$ from (59) and (60) for adiabatic orbits (dashed lines) and diabatic orbits (solid lines), respectively, of Hamiltonians (56) versus scaled energy e.

dominant peaks correspond to the diabatic orbits, and the four small peaks correspond to the adiabatic orbits. For $e = 10^5\,\hbar\omega_0/\bar{\kappa}^2$, the only two peaks correspond to the asymptotic values of $s_i^{\rm dia}(e)/e = T_i^{\rm dia}$, in agreement with the limit (61).

The evidence of diabatic orbits according to the above spin–flip hypothesis had already been observed by Frisk and Guhr [19]. They did, however, not recognize any signatures in their Fourier spectra corresponding to periods of adiabatic orbits involved with MC points, such as we have found them in the four minor peaks of figure 9. Their conclusion was therefore that spin–flips always occur at the MC points. Our results seem to suggest that both kind of dynamics occur. The dominant Fourier peaks are, indeed, those corresponding to the diabatic orbits which undergo spin–flips at the MC points. However, there must also exist a finite probability that the orbits stay on the adiabatic surfaces $H\pm = E$, leading to the smaller peaks positioned at the correct adiabatic quasiperiods $s(e)/e$.

The semiclassical amplitudes required for the trace formula cannot be calculated for the present system, neither using diabatic nor adiabatic orbits. The fully polarized treatment of the spin variables used in the SCL approach is obviously not flexible enough to account for the full dynamics, although the Fourier analysis of the quantum spectra suggests that there is some partial truth to it. A more complete semiclassical description of the spin motions should allow for a balanced mixture of adiabatic and diabatic spin motions.

7. Summary and conclusions

We have derived semiclassical trace formulae for several non-relativistic two- and three-dimensional fermion systems with spin–orbit interactions of Rashba and Thomas types. We have thereby employed the weak-coupling limit (WCL) developed by Bolte and Keppeler

[20] and the strong-coupling limit (SCL) of Littlejohn and Flynn [17] with extensions and justifications of [19, 20].

In the WCL approach, the spatial motion of the particles is taken into account only using the periodic orbits of the system without spin–orbit interaction. The spin motion is included adiabatically via the trace of a spin transport matrix $\mathtt{d}(t)$ which describes the spin precession about the instantaneous magnetic field provided by the spin–orbit interaction. Nevertheless, we found that for a 2DEG in an external magnetic field with and without lateral anharmonic confinement, the WCL yields excellent results. In the free case, for which an exact trace formula can be derived, the semiclassical WCL reproduces the exact leading-order terms both in $\hbar$ and in the spin–orbit coupling constant κ. In the laterally confined case, the gross-shell structure of the coarse-grained quantum level density was very accurately reproduced numerically. From our results it can be seen that in the limit of very large spin–orbit constants κ, the missing higher order terms may restrict the applicability of this method. A particular situation, where the WCL approach misses the effects of the spin–orbit interaction totally, is that where only self-retracing isolated periodic orbits exist, for which the trace of $\mathtt{d}(T_{po})$ only yields a trivial spin degeneracy factor 2.

We have studied the SCL approach for two systems possessing exclusively self-retracing isolated orbits for which the WCL approach fails, namely two- and three-dimensional harmonic oscillators with irrational frequency ratios. In the SCL approach the mode conversion (MC) problem, arising at points in phase space where the spin–orbit interaction locally is zero, imposes severe restrictions, since singularities in the equations of motion and the linear stability analysis of periodic orbits arise at the MC points. However, in the three-dimensional case, which provides a realistic shell model for light atomic nuclei, we found that the leading orbits with shortest periods are free of MC and lead to excellent results of the semiclassical trace formula for the coarse-grained level density, as long as bifurcations of these orbits are avoided. (The latter, when they are sufficiently separated in phase space, can be taken into account using well-developed uniform approximations and do, in principle, not affect the applicability of the SCL approach.)

In the two-dimensional model of an anisotropic quantum dot, the MC problem could not be avoided. By a Fourier analysis of the quantum spectrum, we have provided some support to the diabatic spin–flip hypothesis put forward by Frisk and Guhr [19]. We have to extend their conclusions, though, in the sense that there is evidence for a mixture of both diabatic and adiabatic classical motions on the two spin-polarized energy surfaces $H_{\pm} = E$, whereby the diabatic periods dominate the Fourier spectra. But even in the diabatic spin–flip limit, the semiclassical amplitudes of the trace formula cannot be calculated, and the MC problem therefore remains essentially unsolved. The connection between the existence of MC points and real spin–flip processes should therefore be taken with caution. In order to study the physical relevance of spin–flips in the presence of a spin–orbit interaction, there is a definite need for a better analytical semiclassical treatment of the spin degrees of motion that is free of singularities and allows for a balanced mixture of adiabatic and diabatic spin motions. A new approach [29] in which the MC problem does not arise is presently being developed and will be presented in more detail in a forthcoming paper.

Acknowledgments

We are grateful to J Bolte, S Keppeler, M Langenbuch, M Mehta, M Pletyukhov, O Zaitsev and U Rössler for stimulating discussions. This work has been supported by the Deutsche Forschungsgemeinschaft.

References

[1] Gutzwiller M C 1971 *J. Math. Phys.* **12** 343 and references therein
[2] Cvitanović P (ed) 1992 Chaos focus issue on periodic orbit theory *Chaos* **2**
[3] Gutzwiller M C 1990 *Chaos in Classical and Quantum Mechanics* (New York: Springer)
[4] Berggren K-F and Åberg S (eds) 2001 Quantum chaos Y2K *Phys. Scr.* **T90**
[5] Haake F 2001 *Quantum Signatures of Chaos* 2nd edn (Berlin: Springer)
[6] Balian R and Bloch C 1972 *Ann. Phys., NY* **69** 76
[7] Strutinsky V M 1975 *Nukleonika* **20** 679
Strutinsky V M and Magner A G 1976 *Sov. J. Part. Nucl.* **7** 138
Strutinsky V M, Magner A G, Ofengenden S R and Døssing T 1977 *Z. Phys.* A **283** 269
[8] Berry M V and Tabor M 1976 *Proc. R. Soc.* A **349** 101
Berry M V and Tabor M 1977 *Proc. R. Soc.* A **356** 375
[9] Creagh S C and Littlejohn R G 1991 *Phys. Rev.* A **44** 836
Creagh S C and Littlejohn R G 1992 *J. Phys. A: Math. Gen.* **25** 1643
[10] Creagh S C 1996 *Ann. Phys., NY* **248** 60
Brack M, Creagh S C and Law J 1998 *Phys. Rev.* A **57** 788
[11] Tomsovic S, Grinberg M and Ullmo U 1995 *Phys. Rev. Lett.* **75** 4346
Ullmo D, Grinberg M and Tomsovic S 1996 *Phys. Rev.* E **54** 135
[12] Ozorio de Almeida A M and Hannay J H 1987 *J. Phys. A: Math. Gen.* **20** 5873
[13] Sieber M 1996 *J. Phys. A: Math. Gen.* **29** 4715
Schomerus H and Sieber M 1997 *J. Phys. A: Math. Gen.* **30** 4537
Sieber M and Schomerus H 1998 *J. Phys. A: Math. Gen.* **31** 165
[14] Brack M, Meier P and Tanaka K 1999 *J. Phys. A: Math. Gen.* **32** 331
[15] Brack M and Bhaduri R K 1997 Semiclassical physics *Frontiers in Physics* vol 96 (Reading, MA: Addison-Wesley)
[16] Brack M 2001 *Adv. Solid State Phys.* **41** 459
[17] Littlejohn R G and Flynn W G 1991 *Phys. Rev.* A **44** 5239
[18] Littlejohn R G and Flynn W G 1992 *Phys. Rev.* A **45** 7697
[19] Frisk H and Guhr T 1993 *Ann. Phys., NY* **221** 229
[20] Bolte J and Keppeler S 1998 *Phys. Rev. Lett.* **81** 1987
Bolte J and Keppeler S 1999 *Ann. Phys., NY* **274** 125
[21] Amann Ch 2001 Semiklassische Näherungen zur Spin-Bahn Kopplung *PhD Thesis* Universität Regensburg webpage http://www.bibliothek.uni-regensburg.de/opus-cgi/w3-msql/opus/frontdoor.html?source_opus=29
[22] Brack M and Amann Ch 2001 *Fission Dynamics of Atomic Clusters and Nuclei* eds J da Providência *et al* (Singapore: World Scientific) p 5 (*Preprint* nucl-th/0010047)
[23] Nilsson S G 1955 *Mat.-Fys. Medd. K. Dan. Vidensk. Selsk.* **29**
Mottelson B R and Nilsson S G 1959 *Mat.-Fys. Skr. Dan. Vid. Selsk.* **1**
[24] Goeppert-Mayer M 1949 *Phys. Rev.* **75** 1969
[25] Berry M V and Mount K E 1972 *Rep. Prog. Phys.* **35** 315
[26] Strutinsky V M 1968 *Nucl. Phys.* A **122** 1
[27] Sieber M and Steiner F 1991 *Phys. Rev. Lett.* **67** 1941
Sieber M 1992 *Chaos* **2** 35
[28] Littlejohn R G and Flynn W G 1994 *Ann. Phys., NY* **243** 334
[29] Pletyukhov M, Amann Ch, Mehta M and Brack M 2002 *Phys. Rev. Lett.* at press
[30] Bychkov Y and Rashba E 1984 *J. Phys. C: Solid State Phys.* **17** 6039 and references therein
[31] Darnhofer T, Suhrke M and Rössler U 1996 *Europhys. Lett.* **35** 591
[32] Keppeler S and Winkler R 2002 *Phys. Rev. Lett.* **88** 046401
[33] Brack M and Jain S R 1995 *Phys. Rev.* A **51** 3462
[34] Götz U, Pauli H C and Alder K 1971 *Nucl. Phys.* A **175** 481
[35] Jennings B K, Bhaduri R K and Brack M 1975 *Nucl. Phys.* A **253** 29
[36] Wintgen D 1987 *Phys. Rev. Lett.* **58** 1589
Friedrich H and Wintgen D 1989 *Phys. Rep.* **183** 39
[37] Creagh S C, Robbins J M and Littlejohn R G 1990 *Phys. Rev.* A **42** 1907